

Impacts of Anode Set on the Energy Re-distribution of PB Aluminum Smelting Cells

C. Y. Cheung, C. Menictas, J. Bao*, M. Skyllas-Kazacos, B. J. Welch
School of Chemical Engineering, the University of New South Wales, Sydney NSW 2052, Australia

Keywords: Individual anode current, Thermal modeling, Anode setting

Abstract

Since the introduction of prebaked anodes technology in Hall-Héroult process, anode setting has become one of the routine work practices. As all anodes in different parts of the cell are changed in turn at short regular intervals, the operation is always subject to a different degree of disturbances. This paper presents a dynamic thermal model that can be used to simulate the impact of anode setting on the local thermal balance and hence the overall operating condition by incorporating individual anode current signals as model inputs. This is done by discretizing the bath into multiple subsystems based on the position of each anode. The model can predict the local thermal conditions during the increase of current pick up of a newly replaced anode when based on online measurements of current distribution. A model incorporated with anode current distribution as model inputs can be employed as a foundation for future development of an online fault diagnostic system to help isolating other disturbances, hence improve early detection of impending abnormal conditions.

Introduction

Importance of thermal model

The Hall- Héroult process is a high temperature process takes place in a reduction cell that has a distinctive interdependent nature between the mass and thermal balance. This coupled effect causes a significant dependence of the process performance on the thermal balance. A well-maintained thermal balance allows proper melting of feeds, keeps the ledge in a desired profile, avoids the formation of sludge and thus results in better process efficiency. As the operating conditions have been tightened in recent years due to the needs of optimizing current efficiency and minimizing energy consumption, it becomes more important to keep the thermal balance at a desired window from operation and control perspectives.

During operation, different work practice can take place at different parts of the cell. They give rise to spatial effects on the cell thermal balance that can have influences on the overall process dynamics. These localized variations are hard to detect from online monitoring used in most of the smelter as conventional measurements such as cell voltage, V_{cell} and line current only reflect global cell behaviors. Local thermal imbalance can be resulted in due to routine work practices such as feeding and metal tapping. However, their impacts are not as significant as anode setting.

Anode setting has become a more critical operation as the anode sizes have increased at the expense of liquid bath volume, especially for low superheat operation. When each anode reaches the end of its service life, the anode butt is removed and replaced with a new cold prebaked anode. This causes the breakage of part of the parallel electrical circuit constituted by the anodes and leads

to anode current redistribution, interrupting the thermal balance of the cell. Freeze forms around the cold anode as it acts as an enormous heat sink resulting in deficiency of heat. Thus, additional voltage input is required for melting the freeze. Provided no other abnormalities are occurring during the operation, the current distribution is restored to its previous state once the freeze melts and the newly replaced anode resumes its average current pick up. As each anode in different parts of the cell is changed at short regular intervals, the operation is always subject to a different degree of disturbances, altering the control envelope and decision making limits. It is therefore important to estimate its impact on the local cell thermal balance for better control actions.

Thermal models in literatures

Various thermal models are developed in the past for research, cell development and control purposes. Due to the complexity and the time dependent nature of the process, most of the models developed only focus on parts of the process. The level of detail captured in these models depends on the applications and the speed of the model processing restricted by the computational power available. Distributed parameter models are mainly developed for retrofit and cell design^[1]. They provide high level of detail yet they are not suitable for real time processing such as cell control as substantial simulation time and computational power are often required for one analytical solution. The development of transient lumped parameter models for real time application therefore becomes a better option. They are able to compute the process behavior quickly by solving a set of ordinary differential equations^{[2], [3],[4], [5]}. This type of models takes conventional measurements such as cell voltage and line current as their main model inputs. Manual measurements such as bath temperature are sometimes used to correct the offset and to update the computed states of the cell from time to time. As cell voltage and line current do not reflect local cell conditions, these models are only capable of computing global variations in the process, neglecting any possible spatial variation that may occur due to work practices and localized process dynamics.

Simulate local conditions with new measurement inputs

The lack of available spatial information can be overcome by introducing individual anode currents signal as extra model inputs. Cell voltage and line current are often used as the main inputs for cell monitoring and control because of the harsh environment in the process^{[6], [7]}. Intermittent measurements on the bath such as bath temperature and superheat are also sometimes carried out at a particular location in the cell to monitor the thermal condition of the cell. These measurements are often assumed to be representative for the entire cell for a period of time before the next measurements. They have limited potential to observe dynamic local variation. Unlike the above conventional measurements, individual anode currents reflect the process

dynamics in each current path in terms of path electrical resistance contributed by individual anode process dynamics. They can be measured in real-time in a non-destructive manner as opposed to bath measurements that require direct contact in the corrosive bath and instrumental analysis offsite. They can be used to facilitate online monitoring and fault diagnosis during the occurrence of abnormalities. Its application as model inputs to thermal model can also allow estimation of local cell thermal response when current distribution changes.

The model presented in this paper incorporates individual anode currents as extra model inputs to compute local bath temperature and local ledge thickness in a distributive manner. The use of these additional inputs aims to increase cell observability and detect local thermal variation during different operation such as anode setting. This type of transient models based on individual anode current signal is not available in literatures.

Modeling approach

Model discretization

In order to capture the change of local thermal conditions caused by anode current signals inputs, the bath and the ledge regions are discretized into an array of subsystems based on anode locations. For illustrative purposes, a simplified model topology as viewed from the top of a reduction cell is shown in Figure 1. The topology can be expanded to the number of anodes implemented in different cell technology accordingly.

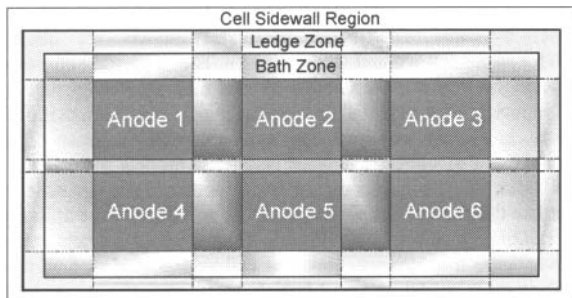


Figure 1 Simplified topology of the discretized bath for thermal modeling for illustrative purposes

Each block in the figure represents a subsystem with their own equations. Benefit from the availability of individual anode current measurements, the vertical subsystems in this approach are not further divided into different horizontal layers of bath and metal, unlike most of the existing models. Instead, each subsystem consists of both the bath layer and the metal layer, with an additional layer of anode block in subsystems where an anode is present. The reason is stated in the following section.

Heat generation in the Hall- Héroult process

The magnitude of individual anode current, I_{an} reflects the total electrical resistance in each path contributed by the bubble layers thickness, anode height, bath conductivity and metal height changes with its wave. On the other hand, it also governs the rate of aluminum production, consumption of alumina concentration in the vicinity of anodes, bubble evolution and anode consumption

via electrochemical reaction. That means the signal itself captures much of the local anode dynamics for instances, the change of anode cathode distance caused by metal waves, the change of bubble thickness etc. in each current path take place. By excluding the voltage drop occurred in the external circuit, V_{ex} carbon cathode, V_{cat} and the heat required for metal production, Q_{Al} , heat generation in each current path via electrical dissipation, Q_{gen} from the surface of the bath to the surface of the carbon cathode can be calculated as follows:

$$Q_{gen} = V_{cell}I_{an} - V_{ext}I_{an} - V_{cat}I_{an} - Q_{Al} \quad (1)$$

By setting the control volume of each subsystem based on relative anode position and the total height of bath and metal, this approach utilizes the advantage of individual anode current, suppressing other model inputs by eliminate the need of calculating electrical resistances based on empirical equations and constants. Each path resistance can also be easily calculated by:

$$R_{path} = \frac{(V_{cell} - V_{ext} - V_{cat} - V_{Al})}{I_{an}} \quad (2)$$

where V_{Al} is the equivalent voltage of metal production. The introduction of individual current signal also allows capturing the electrical resistance contributed by other layers which are difficult to model, such as the formation of bubble and sludge, leading to a more accurate computation of heat generation if abnormal conditions occur.

Model features

By taking cell voltage and individual anode current as model inputs, the model computes heat exchanges (Q_{in} , Q_{out}) between each subsystem based on thermal balances derived from the general heat equation:

$$\frac{d(CT_{subsystem})}{dt} = Q_{in} - Q_{out} + Q_{gen} \quad (3)$$

where C and $T_{subsystem}$ are the thermal conductance and the temperature of the subsystem respectively. The model assumes current only enters the bath via anodes as they have least electrical resistance; the heat generation term only exists in subsystem where anode exists.

The coupled mass and thermal balance

In the presence of ledge, the bath composition in the process can be altered during ledge freezing and melting, caused by the change of a thermal driving force [8]. It is commonly referred as superheat and defined by:

$$\Delta T = T_{bath} - T_{liq} \quad (4)$$

T_{bath} is the bath temperature and T_{liq} liquidus temperature which changes with the bath composition. Under the condition where local thermal imbalance occurs, the superheat at different part of the cell would be difference, consequently causing different degree of ledge melting and freezing. The ledge profile along the

cell is therefore always non-uniform. This coupled phenomenon is computed in the model based on the local heat flows in, $Q_{\text{local in}}$ and local heat flows out $Q_{\text{local out}}$, of each local ledge region.

$$\frac{dM_{\text{ledge, subsystem}}}{dt} = \frac{Q_{\text{local out}} - Q_{\text{local in}}}{\Delta H_f} \quad (5)$$

where ΔH_f is heat of fusion of cryolite.

The change of the total mass of ledge is then used to calculate the change of bath volume that determines the bath height, thus the control volume of each subsystem.

$$\rho_{\text{bath}} \frac{d(h_{\text{bath}} A(\delta_{\text{ledge}}))}{dt} = - \sum \frac{dM_{\text{ledge}}}{dt} \quad (6)$$

It is assumed that the change of the bath volume is only caused by the change of each individual ledge thickness in this model.

The ledge temperature is computed in a similar way as the subsystem temperature with its control volume changes with the corresponding ledge thickness, δ . A sample equation of a thermal balance of the ledge highlighted in red in Figure 2 is present in the following.

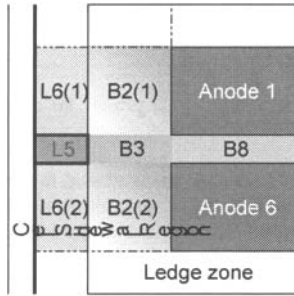


Figure 2 Model topology of computation of ledge temperature

$$\frac{d(\rho C_p V_{L5} T_{L5})}{dt} = \frac{2k_L A_y}{\delta_{L5}} (T_{\text{liq}} - T_{L5}) + \frac{k_{\Sigma} A_y (T_{\text{sidewall}} - T_{L5})}{x(\delta_{L5})} + Q_1 + Q_2 \quad (6)$$

where

$$Q_1 = \begin{cases} \frac{k_L A(\delta_{L5}) \cdot (T_{L6(1)} - T_{L5})}{y} & \delta_{L6(1)} \geq \delta_{L5} \\ \frac{k_L A(\delta_{L6(1)}) \cdot (T_{L6(1)} - T_{L5})}{y} - \frac{k_L A(\delta_{L5} - \delta_{L6(1)}) \cdot (T_{L5} - T_{\text{liq}})}{y} & \delta_{L6(1)} < \delta_{L5} \end{cases} \quad (7)$$

$$Q_2 = \begin{cases} \frac{k_L A(\delta_{L5}) \cdot (T_{L6(2)} - T_{L5})}{y} & \delta_{L6(2)} \geq \delta_{L5} \\ \frac{k_L A(\delta_{L6(2)}) \cdot (T_{L6(2)} - T_{L5})}{y} - \frac{k_L A(\delta_{L5} - \delta_{L6(2)}) \cdot (T_{L5} - T_{\text{liq}})}{y} & \delta_{L6(2)} < \delta_{L5} \end{cases} \quad (8)$$

k_{Σ} is the overall thermal resistance between the ledge and sidewall while k_L is thermal resistance of the ledge. x and y represent the increments between each subsystem in x and y -direction respectively. The model assumes the interface between ledge and the bath are always at liquidus temperature.

Based on the proposed model topology, heat loss from the bath to the top in each subsystem is also simulated. As the temperature gradient is comparatively higher vertically then horizontally, the heat transfer is assumed to be one dimensional.

Anode setting

In the simulation study of anode setting, as the anode is removed along with top crusts and dressing, the top crust term in the thermal balances of the neighboring subsystems is replaced by the air convection term. At the stage of anode removal, the heat exchanges in those subsystems surrounding the removed anode are slightly adjusted to take into account the change of heat transfer in between. When a cold anode is immersed in the bath, it is assumed that solidification of bath only takes place underneath the anode. The dynamic change of it melting and freezing is computed similar to Equation 5.

Results and Discussions

Simulation studies have been performed based on the proposed model of a reduction cell consisting of twenty anode blocks during normal operation and in the early stage of anode setting.

During normal operation

The simulation has been carried out based on certain initial conditions of the reduction cell with the current inputs for all anodes of same initial height are set to be 12.35kA, remained unchanged during the simulation. As the height of anodes continuously decreases due to carbon consumption, the cell condition does not reach steady state even before the anodes reach the end of service life. The bath temperature profile present in Figure 3 is the computed results after twenty hour of simulation. The temperature profile and other simulated results are used as an initial condition to simulate the thermal response of the cell during anode setting. Note that the blocks in the profile are not scale to the geometry applied in the model.

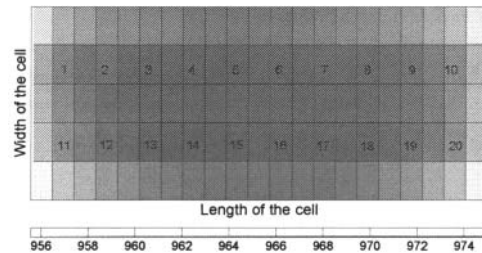


Figure 3 Bath temperature ($^{\circ}\text{C}$) profile of the bath during normal operation

Anode removal

During anode setting, a hot anode butt is firstly removed manually from the bath by a crane. Anode dressing and top crust

surrounding that particular anode are also removed. A large area of the bath is therefore exposed to the ambient air before a new old anode is ready to immerse in the bath. The duration of this stage depends on the manual operation. The simulation result in Figure 4 shows the temperature profile when the bath is exposed to the surrounding for ten minutes after anode 2 is removed.

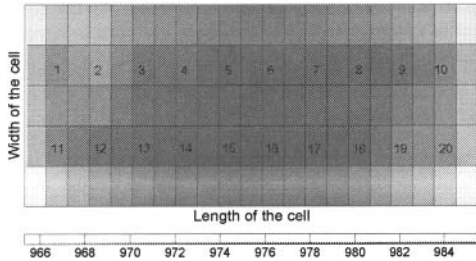


Figure 4 Bath temperature (°C) profile of the bath during anode removal

The local temperatures in the regions near where anode 2 was are comparatively lower than the other part of the bath. This is because a large block of heat is removed from the area and the bath is directly exposed to the air. Decrease in bath temperature is also caused by the breakage of parallel circuit when the anode is removed as no heat generation takes place. This leads to a current redistribution amongst other anodes, generating extra heat via electrical dissipation. As a result, the overall bath temperature increases.

The impact of the duration of anode removal is also studied in the simulation. The plot in Figure 5 shows the change of ledge thickness near anode 2 in every 5 minutes. Although heat loss from the bath during this stage would be a lot smaller when compared with the immersion of a cold anode in the bath, the ledge thickness still increases gradually along with increasing duration. It is therefore important to shorten the removal time in order to minimize the disturbance on the local thermal condition.

Although the current model does not consider the heat loss from the bath due to the falling crust and dressing, the impact of anode removal on the local thermal condition as bath exposed to air is still significant. Based on the proposed modeling approach, the thermal variation can be observed easily.

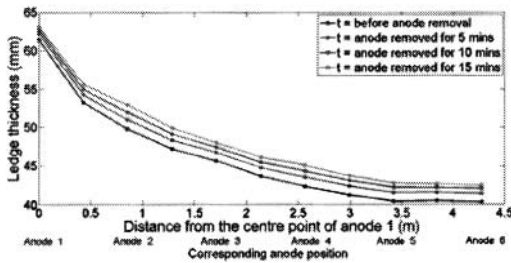


Figure 5 Change of ledge profile near where the anode is removed

A cold anode immersed in the bath

As there is no preheating process for the new anode during anode setting, its temperature is often as low as the ambient temperature. As a result, the new cold anode becomes a large heat sink when it is placed in the bath. This operation creates a significant impact on the cell thermal condition. A simulation study has been conducted to compute the thermal response of the cell in the early stage of anode setting. At this stage, it is assumed that there is no top crust and anode dressing on top of the anode and the surrounding area. The current pickup by the new anode is approximated by a ramp function while other anode currents will change accordingly. Preliminary result of the thermal response of the cell ninety minute after anode setting is shown in Figure 6. The assumption of freeze only form and stays underneath the anode applies in this model.

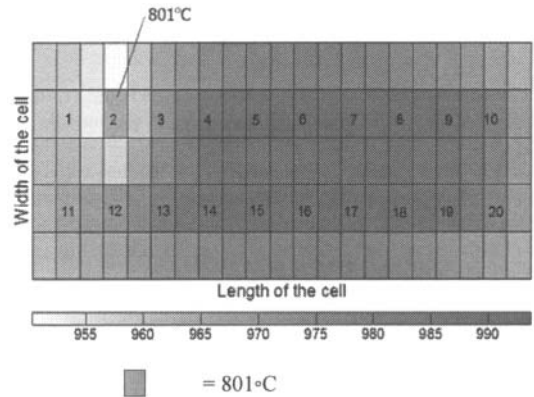


Figure 6 Bath temperature (°C) profile 90 minutes after anode setting

The anode temperature after being placed in the bath for ninety minutes has increased to 801 °C from the initial temperature of 50 °C. The profile shows temperatures at the neighboring region of the cold anode is lower than the rest of the cell yet they are still high compared with the anode temperature. This is due to the energy flow from the other part of the cell carried by the bath velocity which is taken into account by the bath conductivity.

The impact of anode setting on the ledge thickness is quite obvious, as shown in Figure 7. Due to the decrease of superheat when the local bath temperature decreases, the local ledge thickness increases especially at the region close to the cold anode.

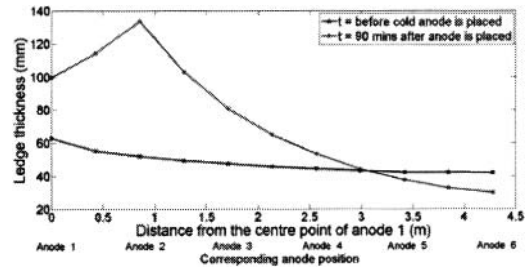


Figure 7 Change of ledge profile near where a new anode is placed in the bath

Conclusion

The thermal model presented in this paper demonstrates its ability to simulate local thermal conditions and local ledge thickness in an aluminum reduction cell in different conditions based on the current distribution.

The introduction of individual anode currents can facilitate cell online monitoring and fault diagnosis in real time. As model inputs, they allow a simpler yet more accurate computation of heat generation in the bath via electrical dissipation. This is different from traditional approaches which electrical resistance of each layer needed to be calculated separately based on theoretical and empirical equations. The model topology is discretized differently from models in literature in order to utilize anode current signal to compute and detect local heat balance and the mutual effect on the local ledge thickness.

This model offers an insight of local cell conditions, allowing estimation of local thermal response during routine work practice such as anode setting. It therefore can provide a foundation of future development of a fault diagnosis system to detect thermal abnormalities at a localized level.

Acknowledgement

This project is supported by the CSIRO Cluster on Breakthrough Technologies for Aluminum Reduction.

Reference

- [1] M. Dupuis, Using ANSYS to model aluminum reduction cell since 1984 and beyond, *Proc. the International ANSYS conference*, Pittsburgh, PA, 2002.
- [2] G. Bearne, The development of aluminum reduction cell process control, *JOM Journal of the Minerals, Metals and Materials Society*, 51(1999), 16-22.
- [3] S. Kolås and T. Støre, Bath temperature and AlF₃ control of an aluminium electrolysis cell, *Control Engineering Practice*, 17(9), 2009, 1035 - 1043.
- [4] E. A. Sorheim and P. Borg, Dynamic model and estimator for online supervision of the alumina reduction cell, *TMS Light Metals*, Las Vegas, Nevada, USA, 1989, 379-384.
- [5] L. Tikasz, R. T. Bui and V. Potocnik, Aluminium electrolytic cells: A computer simulator for training and supervision, *Engineering with Computers*, 10(1994), 12-21.
- [6] H. Kvande and W. Haupin, Cell voltage in aluminum electrolysis: A practical approach, *JOM Journal of the Minerals, Metals and Materials Society*, 52(2000), 31-37.
- [7] P. Homsy, J.-M. Peyneau and M. Reverdy, Overview of process control in reduction cells and potlines, *TMS Light Metals*, Nashville, Tennessee, USA, 2000.
- [8] M. Iffert, M. Skyllas-Kazacos and B. Welch in *Challenges in Mass Balance Control*, Vol. 2005.